

# Modeling the Differential Rate for Signal Interactions in Coincidence with Noise Fluctuations or Large Rate Backgrounds

Xinran Li\*

*Lawrence Berkeley National Laboratory, Berkeley, CA 94720, USA*

Matt Pyle

*Lawrence Berkeley National Laboratory and  
University of California Berkeley, Berkeley, CA 94720, USA*

Bernard Sadoulet

*University of California Berkeley, Berkeley, CA 94720, USA*  
(Dated: November 19, 2024)

The characteristic energy of a relic dark matter interaction with a detector scales strongly with the putative dark matter mass. Consequently, experimental search sensitivity at the lightest masses will always come from interactions whose size is similar to noise fluctuations and low energy backgrounds in the detector.

In this paper, we correctly calculate the net change in measured differential rate due to signal interactions that overlap in time with noise and backgrounds, accounting for both periods of time when the signal is coincident with noise/backgrounds and for the decreased amount of time in which only noise/backgrounds occur. Previous experimental searches have not accounted for this second fundamental effect, and thus either vastly overestimate their experimental search sensitivity (very bad) or use ad hoc conservative cuts which can underestimate experimental sensitivity (not ideal). We find that the detector response to dark matter can be trivially and conservatively understood as long as the true probability of dark matter pileup is small.

We also show that introducing random events in the continuous raw data stream (a form of “salting”) provides a correct and practical implementation that correctly accounts for the decreased live time available for noise fluctuations and background events out of coincidence with a true dark matter signal.

## I. INTRODUCTION

Detectors for direct detection of particle dark matter (DM) record signals in time streams. In most cases, a triggering algorithm is applied to select potentially interesting signals from the continuous stream. Then, the signals are processed to estimate the differential rate as a function of measured energy,  $\frac{dR}{dE'}$ , and generate a dark matter sensitivity estimate. Detectors have noise and backgrounds, and an event with true energy deposition  $E$  produces a signal reconstructed at energy  $E'$  with a probability  $f(E'|E)$ . Understanding  $f(E'|E)$ , i.e., the

detector energy response, is the core of an experiment.

For light mass DM, where the mass of the DM,  $M_{\text{DM}}$ , is much less than the mass of the target nuclei in the detector,  $M_{\text{N}}$ , the energy deposited in an elastic two-body nuclear scattering interaction is  $E \lesssim \frac{2M_{\text{DM}}^2 v_{\text{esc}}^2}{M_{\text{N}}}$  where  $v_{\text{esc}}$  is the escape velocity for the Milkyway. This  $M_{\text{DM}}^2$  dependence means that signals for the lowest  $M_{\text{DM}}$  are near or even below the trigger threshold,  $E'_T$ . Specifically, it is possible that a DM interaction with a true energy deposition below the trigger threshold ( $E < E'_T$ ) could occur in coincidence with a positive random noise fluctuation,  $\delta E'$ , and thus be boosted above the trigger threshold,  $E + \delta E' = E' > E'_T$ . We want to correctly derive the change in the measured differential rate spectrum,  $\frac{dR}{dE'}$ , due to these in-

---

\* xinranli@lbl.gov

teractions so that we can correctly account for this sensitivity in our searches.

As we will elaborate in section IV, the net change in  $\frac{dR}{dE'}$  is due to both:

- the signal interacting with the detector in coincidence with a large noise fluctuation or other background.
- a decrease in the rate of large noise fluctuations/backgrounds that are non-coincident with signal interactions.

Not accounting for this latter effect can lead to unphysical overestimation of the sensitivity. For example, an experiment must obviously have no sensitivity to a hypothetical interaction that deposits identically zero true energy in the detector. However, this  $E = 0$  event will have a probability of being in coincidence with background fluctuations  $\delta E' > E'_t$  and thus will naively be boosted above the trigger threshold. Only after accounting for both of the physical effects above will  $\frac{dR}{dE'}$  not have unphysical sensitivity to  $E = 0$  interactions (Sec. II B 2).

To suppress these most blatant unphysical consequences of incorrectly estimating net changes in  $\frac{dR}{dE'}$ , previous light dark matter direct detection searches [11, 14, 21], restricted the allowable noise boosting usually to  $\delta E' = E' - E < 3\sigma$ , where  $\sigma$  is the baseline energy RMS. However, the lack of a rigorous theoretical underpinning led to problematic ambiguity (is  $\delta E' < 2\sigma$  too conservative? Does  $\delta E' < 4\sigma$  overestimate sensitivity?). Thus, only a deeper understanding of how to correctly model the coincidence of signal and noise/background rates allows one to correctly estimate the actual experimental sensitivity.

Though we were motivated to understand noise boosting originally in phonon detectors, this is a general problem present in all detector technologies and in any search where the signal is commingled, coincident, and of similar magnitude to the noise and background events. For example, a light mass dark matter search with a p-type point contact germanium ionization detector [20] attempted to search for noise-boostered signals by simply Gaus-

sian smearing the expected dark matter spectrum without correctly restricting the boost and potentially overestimated their dark matter sensitivity for low mass DM. In detectors where the signal energy quanta are resolved, for example, skipper CCDs[15, 16], noble liquid time projection chambers[1, 4, 12], and phonon sensors with Neganov-Trofimov-Luke (NTL) amplification[6], noises on the baseline are truly negligible at the trigger level. But a high rate of physical background events (i.e. charge leakage) can boost small signals as well when they are in coincidence; for example, a single  $e^-$  excitation dark matter signal can occur in coincidence with a single  $e^-$  charge leakage event in a noble two-phase time projection chamber (TPC) and produce a  $2e^-$  above trigger event.

We will first examine a simple scenario of ideal integrating detectors, and introduce the concept of the net differential signal response  $\Delta f(E'|E) = f(E'|E) - f(E'|0)$  in Sec. II. In Sec. III, we will discuss the subtlety of estimating  $\Delta f(E'|E)$  when the experimental search data is contaminated with an unknown rate of signal interactions and find that as long as the signal pileup rate is negligible, a conservative interaction limit that is guaranteed to have a larger expectation than the true signal rate can be estimated using the net differential response. In Sec. IV, we will generalize the discussion to continuous DM interaction spectra and demonstrate the conservativeness in a toy example. Next, we will generalize these concepts to experiments with continuous data streams and timing information in Sec. V. We will refer to these detectors as “analog detectors”. In such analog devices, the concept of a signal interaction being in “coincidence” with a large noise fluctuation is qualitative. More rigorously, we should say that the time difference between a large noise fluctuation and the dark matter event is small. Finally, in Sec. VI, we will show that introducing a known rate of artificial random signal events in the continuous raw data stream (pretrigger “salting”) correctly estimates the net differential response.

## II. DERIVATION FOR A DISCRETIZED INTEGRATING DEVICE

In this section, we will suppress these subtleties and think instead about the behavior of an idealized integrating time-discretized detector like a CCD. In an idealized CCD, for instance, the total integrated charge deposited in the pixel is measured every  $\Delta t$ , after which the pixel is reset and begins to integrate the charge for the next discrete measurement. All measurements are recorded without a trigger. We will assume that the time scale for energy deposition is instantaneous and the time to measure and reset is infinitesimal.

### A. Single Dirac-Delta True Energy Deposition

The second simplification we will make, initially at least, is that each and every interaction event produces an identical true energy signal in the sensor,  $E_s$ . Beyond being easier to understand, this scenario has physical relevance since it corresponds to bosonic dark matter absorption.

With these two simplifications, we can calculate the expected differential rate of the measured energy  $E'$  in terms of:

- $f(E'|E = n_s E_s) \equiv f(E'|n_s E_s)$ : the probability distribution of measured energy,  $E'$ , in the time interval  $\Delta t$  given a true deposited energy of  $E = n_s E_s$  from  $n_s$  signal interactions occurring in the same time interval.
- $f(E'|E = 0) \equiv f(E'|0)$ : the probability distribution of measured energy,  $E'$ , in the time interval  $\Delta t$  with no signal interactions in the same time interval. This is a subgroup of the previous definition and is the energy point spread function.
- $P(n_s|\lambda_s = R_s \Delta t)$ : the Poissonian distribution for having  $n_s$  events within a time  $\Delta t$  with an average number of interactions

$\lambda_s$  or equivalently an interaction rate of  $R_s$ .

Please note a few things. First,  $f(E'|n_s E_s)$  and  $f(E'|0)$  are highly related. The first expression is the convolution of the second term with a delta-function at true energy  $n_s E_s$ , correcting for possible response nonlinearities. For a perfectly linearly idealized integrating device where the energies of all the events that occur within the  $\Delta t$  time bin just simply add

$$f(E'|n_s E_s) = f(E' - n_s E_s|0) \quad (1)$$

Another way to obtain  $f(E'|n_s E_s)$  is to add  $n_s$  signals with energy  $E_s$  in each integration time  $\Delta t$ . This is the basic form of **salting** that only applies to the simple discretized detector scenario because it requires the time integration intervals to be fixed in time and width.

Using these distributions, we can then write the expected signal rate  $\frac{dR}{dE'}$  as

$$\begin{aligned} \frac{dR}{dE'}(E'|S(E_s, R_s)) &= \frac{1}{\Delta t} f(E'|S(E_s, R_s)) \\ &= \frac{1}{\Delta t} \sum_{n_s=0}^{\infty} P(n_s|R_s \Delta t) f(E'|n_s E_s) \end{aligned} \quad (2)$$

We use  $S(E_s, R_s)$  to represent the signal model. For simplicity, in the later sections, the parameters for the signal model in context will only be explicitly written out once, and then the model will be noted as  $S$ . This notation allows us to easily generalize to more complex signal models, which can produce a continuum of true energy depositions, like DM scattering (see Sec. IV).

We explicitly highlight the seemingly obvious relationship between the measured differential rate and the probability distribution of the measured energy,  $\frac{dR}{dE'}(E'|S) = \frac{1}{\Delta t} f(E'|S)$ . In particular, this relationship means that  $\Delta t \int dE' \frac{dR}{dE'}(E'|S) = 1$ . By contrast, the integral of the differential rate of the signal with respect to the true energy deposition,  $\frac{dR}{dE}(E|S)$ , is  $\Delta t \int dE \frac{dR}{dE}(E|S) = \lambda$ , and is thus **not** a probability distribution. To gain a deeper understanding for this difference, we look at the two limiting cases. When there is no signal interaction at all,  $\Delta t \int dE \frac{dR}{dE}(E|S) = \lambda_s = 0$ . However, the measured differential rate is clearly

non-zero; it's a measure of the noise and backgrounds. On the other hand, when  $\lambda \gg 1$ , there is significant pileup of multiple signal interactions in every bin and  $\frac{dR}{dE'}$  bears little resemblance to  $\frac{dR}{dE}$ .

Returning to 2, we split off and rewrite the  $n_s = 0$  term using the fact that  $\sum_{n_s=0}^{\infty} P(n_s) = 1$ , and find

blance to  $\frac{dR}{dE}$ .

$$\begin{aligned} \frac{dR}{dE'}(E'|S) &= \frac{1}{\Delta t} f(E'|0) \left( 1 - \sum_{n_s=1}^{\infty} P(n_s|R_s\Delta t) \right) + \frac{1}{\Delta t} \sum_{n_s=1}^{\infty} P(n_s|R_s\Delta t) f(E'|n_s E_s) \\ &= \frac{dR}{dE'}(E'|0) \left( 1 - \sum_{n_s=1}^{\infty} P(n_s|R_s\Delta t) \right) + \frac{1}{\Delta t} \sum_{n_s=1}^{\infty} P(n_s|R_s\Delta t) f(E'|n_s E_s) \end{aligned} \quad (3)$$

since  $\frac{dR}{dE'}(E'|0) = \frac{1}{\Delta t} f(E'|0)$ .

Eq. 3 shows that signal interactions affect  $\frac{dR}{dE'}$  in two distinct ways, **both of which must be accounted for**. The second term,  $\frac{1}{\Delta t} \sum_{n_s=1}^{\infty} P(n_s|R_s\Delta t) f(E'|n_s E_s)$ , accounts for the change in the differential rate distribution from those time periods which have one or more signal interactions. The  $\frac{dR}{dE'}(E'|0) (1 - \sum_{n_s=1}^{\infty} P(n_s|R_s\Delta t))$  term, by contrast, accounts for the fact that as  $R_s$  increases, there are fewer time periods without a signal interaction; there are fewer time periods that are solely noise. In other words, the presence of signal interactions decreases the live time available for pure noise fluctuations to be recorded.

Grouping terms in eq. 3 together by  $P(n_s|R_s\Delta t)$ , we find that

$$\begin{aligned} \frac{dR}{dE'}(E'|S) &= \frac{dR}{dE'}(E'|0) \\ &+ \frac{1}{\Delta t} \sum_{n_s=1}^{\infty} P(n_s|R_s\Delta t) (f(E'|n_s E_s) - f(E'|0)) \end{aligned} \quad (4)$$

or equivalently by multiplying through by  $\Delta t$

$$\begin{aligned} f(E'|S) &= f(E'|0) \\ &+ \sum_{n_s=1}^{\infty} P(n_s|R_s\Delta t) (f(E'|n_s E_s) - f(E'|0)) \end{aligned} \quad (5)$$

Under the assumption that there is minimal

signal pileup,  $R_s\Delta t \ll 1$ , this simplifies drastically to

$$\begin{aligned} \frac{dR}{dE'}(E'|S) &= \frac{dR}{dE'}(E'|0) + R_s (f(E'|E_s) - f(E'|0)) \end{aligned} \quad (6)$$

or equivalently

$$\begin{aligned} f(E'|S) &= f(E'|0) + R_s \Delta t (f(E'|E_s) - f(E'|0)) \end{aligned} \quad (7)$$

When written in this way, the term  $R_s (f(E'|E_s) - f(E'|0))$  should be thought of as the net change of the differential rate due to a signal interaction with rate  $R_s$  and energy  $E_s$ . We define

$$\Delta f(E'|E_s) \equiv f(E'|E_s) - f(E'|0) \quad (8)$$

as the ‘‘net differential response’’ of the detector to an event of true energy  $E_s$ .

Eq. 6 (and its non-linear generalization in Eq. 4) is the core insight of this paper. It describes how a signal that is overlapping with background and noise affects the experimentally measured differential rate,  $\frac{dR}{dE'}(E'|S)$ . Most importantly, correct modeling of the  $\Delta f(E'|E_s)$  must occur no matter the statistical technique ultimately used to estimate experimental search sensitivity.

## B. A Variety of Test Cases

We will discuss a series of intuitive test cases to demonstrate that Eq. 6 and their DM high rate generalizations (Eq. 4) should be used rather than a bad expression later shown as Eq. 9 in any analysis where there is a significant noise/background event rate that overlaps with the signal.

### 1. Bosonic DM search with a Gaussian random noise

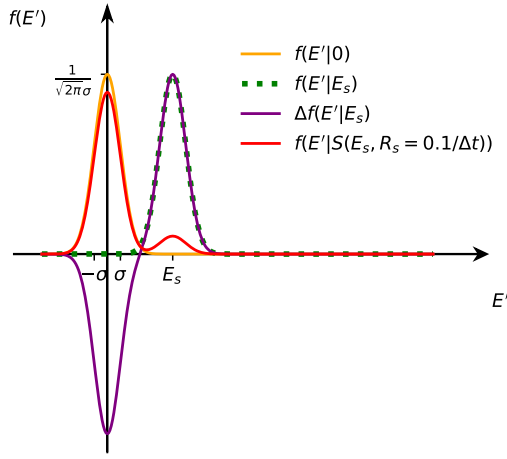


FIG. 1. Probability distribution functions for when  $f(E', 0)$  (yellow) is Gaussian distributed noise. The net change  $\Delta f(E'|E_s)$  (purple) is  $f(E'|E_s)$  (dashed green) subtracted by  $f(E', 0)$ . The DM signal energy  $E_s = 5\sigma$ , where  $\sigma$  is the Gaussian RMS. The signal rate  $R_s = 0.1/\Delta t$ .

We will start with the ideal scenario, a detector for bosonic DM absorption with Gaussian noise fluctuations. In Fig. 1, there are 2 peaks visible in  $f(E'|S(E_s = 5\sigma, R_s = 0.1/\Delta t))$  (red). The large peak centered at  $E' = 0$  consists of time frames that are not in coincidence with a signal interaction; they are due to noise-only time frames. The peak centered at  $E' = E_s$  consists of time frames that have a DM interaction in coincident with the noise.

Notice that the rate of events around zero is slightly less for  $f(E'|S)$  than  $f(E'|0)$  because the former is only those noise events that are anticoincident with the DM. Those coincident with the DM have been up-shifted to being centered around  $E_s$ . This is a physical effect represented by the  $f(E'|0) (1 - \sum_{n_s=1}^{\infty} P(n_s|R_s\Delta t))$  Eq. 3 or equivalently the  $-R_s\Delta t f(E'|0)$  term in Eq. 7.

In experiments like LZ [1], CDMS-II [5], SuperCDMS Soudan [6], etc., the second term is not included because  $f(E'|0)$  has no or very minimal overlap with  $f(E'|E_s)$ . Thus, there exists an analysis threshold that is above nearly the entirety of  $f(E'|0)$  while being below the majority of  $f(E'|E_s)$ . Consequently, neglecting the decrease in the noise-only event rate has no scientific significance in those experiments.

### 2. Searches for Dark Matter where $M_{DM} \rightarrow 0$

As the mass of dark matter,  $M_{DM}$ , approaches 0, the maximum possible energy transferred to the detector also approaches zero,  $E_s \rightarrow 0$ . As such, a necessary but certainly not sufficient condition for a valid DM search analysis technique is that it has no sensitivity to DM interactions in the limit as  $M_{DM} \rightarrow 0$ . Notice that eq. 7 naturally satisfies this condition

$$\begin{aligned} f(E'|S(E_s \rightarrow 0, R_s)) &= f(E'|0) + R_s\Delta t(f(E'|E_s \rightarrow 0) - f(E'|0)) \\ &= f(E'|0) \end{aligned}$$

In this limit, the measured distribution  $f(E'|S)$  is by construction independent of  $R_s$ , and thus, the experiment has absolutely no sensitivity to DM. By contrast, [11, 14, 21] did not account for decreased noise only live time and thus incorrectly assumed that the sensitivity of their measured differential rate to a signal was

$$\frac{dR_{\text{bad}}}{dE'}(E'|S(E_s, R_s)) = \frac{dR}{dE'}(E'|0) + R_s f(E'|E_s)$$

or expressed by the measurement probability distribution as

$$f_{\text{bad}}(E'|S(E_s, R_s)) = f(E'|0) + R_s \Delta t f(E'|E_s) \quad (9)$$

This expression is clearly an ill-defined probability distribution, as the total probability is no longer conservative. Additionally, in the limit of  $E_s \rightarrow 0$ , this incorrect formulation calculates

$$\begin{aligned} f_{\text{bad}}(E'|S(E_s \rightarrow 0, R_s)) \\ &= f(E'|0) + R_s \Delta t f(E'|E_s \rightarrow 0) \\ &= f(E'|0)(1 + R_s \Delta t) \end{aligned}$$

a dependence of the differential rate on  $R_s$ . This is clearly unphysical. It falsely claims that the number of high-energy noise events increases with the dark matter interaction rate, even though these interactions deposit zero energy. To suppress this issue, each of the analyses that used Eq. 35, a generalized version of Eq. 9, added ad-hoc “conservative” constraints to limit their sensitivity to suppress this unphysical sensitivity. In particular, in [11], the authors required that a dark matter event could not be noise boosted by more than  $3\sigma$  when they had a  $4.5\sigma$  trigger threshold to explicitly suppress this unphysical sensitivity to zero energy interactions. However, it bears emphasizing that these ad-hoc suppression techniques are quite problematic because it’s unclear precisely how strong these ad-hoc constraints must be to entirely remove the unphysical and overestimated experimental sensitivity that comes from using the incorrect Eq. 9 instead of the correct Eq. 7.

### 3. Signal search with a high rate calibration peak

The second scenario to consider is when an additional high-rate calibration source hits the detector during the experimental search. For example, in the CPDv1 DM search [11], a  $^{55}\text{Fe}$  x-ray calibration source was hitting the detector during the DM search. To be explicit, we assume this calibration source has a true energy,  $E_{\text{cal}}$ , and a rate of  $0.2/\Delta t$ , so that 20% of the integration windows have a calibration

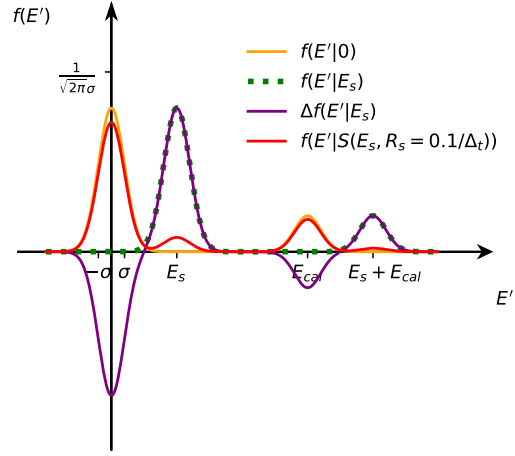


FIG. 2. Same probability distributions as Fig. 1 but assuming a non-Gaussian baseline distribution (yellow) which includes a calibration source at  $E_{\text{cal}}$  and rate  $R_{\text{cal}} = 0.2/\Delta t$ . The signal  $S$  is the same as in Fig. 1

pulse. With this in mind, various probability distributions have been drawn in Fig. 2. In fig. 2, the red  $f(E'|S)$  (where there is DM hitting the detector) has four peaks:

- a peak centered at  $E' = 0$ : these are from noise-only time frames with neither a calibration photon nor a DM interaction. Compared to the yellow no-DM spectrum, the noise peak is suppressed by a factor of  $(1 - R_s \Delta t)$  as we expect from Eq. 6. Compared to the no-DM, no-calibration spectrum in Fig. 1, the rate is suppressed by  $\sim (1 - R_s \Delta t)(1 - R_{\text{cal}} \Delta t)$ .
- a peak centered at  $E' = E_s$ : these are time frames that have a DM interaction but no calibration photon. The total rate here is  $R_s(1 - R_{\text{cal}} \Delta t)$
- a peak centered at  $E' = E_{\text{cal}}$ : these are time frames that have a calibration photon but no DM interaction. This peak has been suppressed by a factor of  $(1 - R_s \Delta t)$  compared to the no DM scenario per our intuition from Eq. 6. The total rate here is  $R_{\text{cal}}(1 - R_s \Delta t)$ .

- a very small peak centered at  $E' = E_{\text{cal}} + E_s$ : these are time frames where both a calibration photon and a DM interaction have occurred in coincidence. This peak has an integrated rate of  $R_s(R_{\text{cal}}\Delta t)$ .

Notice that just like in the first case with Gaussian noise, the peaks at 0 and  $E_{\text{cal}}$  have slightly less total rate in  $f(E'|S)$ (red) than  $f(E'|0)$ (yellow), again, due to the DM-coincident time frames being shifted to the peaks at  $E_s$  and  $E_{\text{cal}} + E_s$ , respectively.

In principle, **one could do a DM search only looking at the coincidence peak between the calibration source and the DM at  $E_{\text{cal}} + E_s$** . However, the sensitivity of such a search will likely be worse than one looking for the peak at  $E_s$  for a few reasons. First, the expected rate of the peak at  $E_s$  is  $\frac{1-R_{\text{cal}}\Delta t}{R_{\text{cal}}\Delta t}$  times the peak at  $E_{\text{cal}} + E_s$ , where  $R_{\text{cal}}\Delta t \ll 1$ . Secondly, a  $E_s + E_{\text{cal}}$  peak search has identical noise contamination as the  $E_s$  peak; noise-boosted calibration-only events will contaminate the calibration + DM signal, just like noise-only events contaminate the DM-only events. Third, the resolution of a high energy peak in real detectors is always worse than the baseline resolution due to statistical fluctuations and position-dependent effects. Finally, in real analog detectors, coincidence is a much more qualitative concept, and thus, the response is much more

complicated (see Sec. V).

We explicitly highlight this scenario for a few reasons. First, our derivation of the net signal response (Eq. 6) doesn't distinguish between "noise" and "backgrounds". Both are things that occur in coincidence with signal and thus must be treated similarly. Secondly, this is the extreme limit of a noise distribution with a non-Gaussian, non-monotonic tail. For example, a constant energy EMI glitch would have all the same effects as a calibration source. The key here is that Eq. 6 allows us to correctly understand and model how a dark matter signal would impact the measured differential rate in experiments with non-Gaussian non-monotonic measured noise and background spectra.

#### 4. Effect of slowly varying non-Gaussian noise tails

Next, we consider the scenario with a non-Gaussian, monotonically decreasing noise tail of unknown origin. This scenario is extremely pertinent since the current generation of light mass DM searches based on cryogenic calorimeters measures a poorly understood near threshold background excess of this type[3, 11, 18].

For concreteness, we will model this scenario with an exponential plus a flat background, which accounts for the low energy excess backgrounds and environmental radioactive backgrounds, respectively. These backgrounds have then been smeared by Gaussian noise:

$$f(E'|0) = \frac{1 - \Delta t(\alpha\tau + \beta E_{\text{max}})}{\sqrt{2\pi}\sigma} e^{-\frac{E'^2}{2\sigma^2}} + \frac{\Delta t}{\sqrt{2\pi}\sigma} \int_0^\infty \left( \alpha e^{-E/\tau} + \beta H(E_{\text{max}} - E) \right) e^{-\frac{(E' - E)^2}{2\sigma^2}} dE \quad (10)$$

where  $H(\cdot)$  is the Heaviside step function, limiting the maximum energy of the flat background to  $E_{\text{max}}$ , and the first Gaussian term accounts for the pure noise frames in the discretized detector such that  $f(E'|0)$  integrates to unity.

An example of this scenario is shown in Fig.3. In the tail region of the noise spectrum, the sensitivity of the differential rate to dark matter,

the net response curve (purple in Fig. 3), is found to be significantly suppressed compared to  $f(E'|E_s)$ (dashed green). This is due to the fact that for small DM energy depositions,  $E_s$ , the net response (Eq. 6) is proportional to the slope of  $f(E'|0)$ ; or equivalently, the vast majority of our reach will occur at where  $\frac{d^2 R}{dE'^2}$  is large. **In fact, in the extreme limit of a**

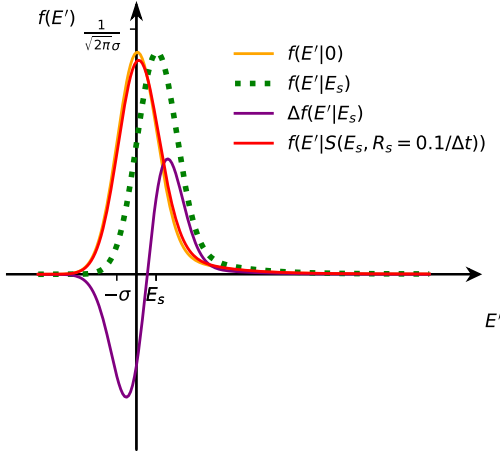


FIG. 3. Same probability distributions as Fig. 1 but assuming a non-Gaussian noise following Eq. 10.  $\alpha = 0.1/\Delta t/\sigma$ ,  $\beta = 5 \times 10^{-4}/\Delta t/\sigma$ ,  $\tau = 2\sigma$ . The signal model here represents a case with low DM energy, where  $E_s = \sigma$  and  $R_s = 0.1/\Delta t$ .

**perfectly flat background, there would be absolutely zero sensitivity to signal in this portion of the spectrum.**

Again, the historically used, but incorrect, rate model of Eq. 35 tends to drastically overestimate signal sensitivity in this critical noise scenario, largely invalidating the use of ad-hoc conservative cuts to suppress the unphysical sensitivity in these searches. It strongly motivates the use of the correct net differential signal response function in future experiments with such backgrounds so that the actual sensitivity can be correctly estimated.

### III. ESTIMATING THE SIGNAL RATE

Now that we understand theoretically how  $f(E')$ , and equivalently  $\frac{dR}{dE'}$ , varies with a known signal rate  $R_s$  of true energy depositions  $E_s$  in the linear (Eq. 6) and non-linear regimes (Eq. 4), we can attempt to statistically estimate an unknown measured signal rate in experimental search data.

The first step, of course, is to simply measure the potentially signal contaminated differential rate,  $\widehat{\frac{dR}{dE'}}(E'|S(E_s, \lambda_s = R_s \Delta t))$ , where the  $S$  explicitly highlights that the measured search data is potentially contaminated by an unknown signal with rate  $R_s$  and true energy deposition  $E_s$  while the ‘ $\wedge$ ’ communicates that this is a statistical estimator. Specifically, we can count the number of measurements,  $N_{E'}$ , with an estimated energy  $E'$  within the range of  $[E' - \frac{\Delta E'}{2}, E' + \frac{\Delta E'}{2}]$  over a time  $T_{\text{total}}$ . In the limit of small energy intervals, the estimator becomes

$$\begin{aligned} \widehat{\frac{dR}{dE'}}(E'|S) \\ \equiv \lim_{\Delta E' \rightarrow 0} \frac{N_{E'}([E' - \frac{\Delta E'}{2}, E' + \frac{\Delta E'}{2}])}{\Delta E' T_{\text{total}}} \end{aligned} \quad (11)$$

This estimator and the related estimator for  $\hat{f}(E'|S)$  are both unbiased and consistent with the true value [19] since their expectation matches the true value and therefore

$$\langle \widehat{\frac{dR}{dE'}}(E'|S) \rangle \Delta t = \langle \hat{f}(E'|S) \rangle = f(E'|0) + \sum_{n_s=1}^{\infty} P(n_s|\lambda_s) (f(E'|n_s E_s) - f(E'|0)) \quad (12)$$

where the second equality follows from Eq. 5. To generate an unbiased and consistent estimator of  $\lambda_s = R_s \Delta t$  from Eq. 12 clearly requires an additional estimation of background

+ noise distribution **without any potential signal contamination**,  $f(E'|0)$ . If this is possible, then  $\hat{f}(E'|n_s E_s)$  can be generated either by shifting the distribution in the case of



ideal linear integrating detectors,  $\hat{f}(E'|n_s E_s) = \hat{f}(E' - n_s E_s|0)$  or via salting methods (Eq. 1). With this additional knowledge,  $\hat{\lambda}_s(E')$  is the solution of

$$\begin{aligned} \hat{f}(E'|S) &= \hat{f}(E'|0) \\ &+ \sum_{n_s=1}^{\infty} P(n_s|\hat{\lambda}_s) \left( \hat{f}(E'|n_s E_s) - \hat{f}(E'|0) \right) \end{aligned} \quad (13)$$

which in the small pileup limit becomes

$$\hat{R}_s(E'|E_s)\Delta t = \hat{\lambda}_s(E') = \frac{\hat{f}(E'|S) - \hat{f}(E'|0)}{\hat{f}(E'|E_s) - \hat{f}(E'|0)} \quad (14)$$

where we've explicitly highlighted that  $\hat{R}_s(E'|E_s)$  is a function of  $E'$ . More complex estimators can be constructed by an optimal weighted integration of  $\hat{R}_s$  over a range of  $E'$  or even using maximum likelihood methods, but they basically share the same features as Eqs. 13 and 14.

#### A. The difficulties of measuring $f(E'|0)$

Unfortunately, in a large class of experiments, it is impossible to “turn off” the DM interaction signal to directly measure  $f(E'|0)$ . High mass dark matter experiments like the noble gas 2 phase TPCs, for example, depend upon a wealth

of event information (ionization and scintillation signal amplitudes, position information) and an enormous amount of calibration data to both separate the majority of backgrounds and model the residual overlapping background  $f(E'|0)$ . Unfortunately, the current generation of light mass dark matter experiments have minimally understood indistinguishable backgrounds (charge leakage [7, 9], dark counts [4, 8], low energy event excess [2, 3, 11, 13]) and thus an understanding of  $f(E'|0)$  is currently impossible.

#### B. Measuring the net differential response

While in many cases  $f(E'|0)$  is not directly estimable and thus a background subtracted signal rate is impossible, one can still estimate the net differential response  $\Delta f(E'|E_s) \equiv f(E'|E_s) - f(E'|0)$  (Eq. 8) from potentially contaminated search data in **the no pileup limit**.

To prove this let us take the probability distribution,  $f(E'|S)$ , that is potentially contaminated by the signal  $S(E_s, \lambda_s)$ , and generate the distribution  $f(E'|S + n_s E_s)$  either by shifting the distribution in the case of ideal linear integrating detectors,  $f(E'|S + n_s E_s) = f(E' - n_s E_s|S)$  or by explicitly adding a true energy deposition of  $n_s E_s$  to the search data before measurement via salting (Eq. 1). Following from Eq. 12, we can relate these boosted signal contaminated search distributions to that of the boosted background-only distributions:

$$f(E'|S + n_s E_s) = f(E'|n_s E_s) + \sum_{m_s=1}^{\infty} P(m_s|\lambda_s) (f(E'|m_s + n_s E_s) - f(E'|n_s E_s)) \quad (15)$$

Flipping Eqs. 12 and 15 to write  $f(E'|0)$  and  $f(E'|n_s E_s)$  in terms of these measurable search distributions and a higher order signal pileup residuals, we find

$$f(E'|0) = f(E'|S) - \sum_{m_s=1}^{\infty} P(m_s|\lambda_s) (f(E'|m_s E_s) - f(E'|0)) \quad (16)$$

and

$$f(E'|n_s E_s) = f(E'|S + n_s E_s) - \sum_{m_s=1}^{\infty} P(m_s|\lambda_s) (f(E'|n_s + m_s E_s) - f(E'|n_s E_s)) \quad (17)$$

which we can then use to rewrite the unmeasurable net differential sensitivities in Eq. 12 in terms of measurable differences between signal contaminated distributions and unmeasurable signal pileup residuals:

$$f(E'|S) = f(E'|0) + \sum_{n_s=1}^{\infty} P(n_s|\lambda_s) (f(E'|S + n_s E_s) - f(E'|S)) - \sum_{n_s=1}^{\infty} \sum_{m_s=1}^{\infty} P(n_s|\lambda_s) P(m_s|\lambda_s) [f(E'|(m_s+n_s)E_s) - f(E'|n_s E_s) - f(E'|m_s E_s) + f(E'|0)] \quad (18)$$

If the unknown average signal interaction number in each time bin,  $\lambda_s = R_s \Delta t$ , is **already** known to be  $\ll 1$ , then Eq. 18 can be Taylor expanded to first order  $\lambda_s$  and we find

$$\begin{aligned} f(E'|S) &= f(E'|0) + \lambda_s (f(E'|S + E_s) - f(E'|S)) \\ &= f(E'|0) + \lambda_s \Delta f(E'|S + E_s) \end{aligned} \quad (19)$$

where  $\Delta f(E'|S + E_s) \equiv f(E'|S + E_s) - f(E'|S)$  is the measurable net differential signal sensitivity with potential signal contamination. In other words, Eq. 19 specifically shows that signal contamination doesn't significantly affect the estimate of the net differential sensitivity in the no-pileup regime.

### C. Conservative upper bound in the no-pileup regime

Using the result of the previous section, we can derive in the no-pileup regime a conservative upper bound on the presence of a signal,  $\hat{R}_{\text{lim}}$ , which requires no understanding of the noise, backgrounds and possibly contaminating signals S.

A conservative upper bound,  $\hat{R}_{\text{lim}}(E'|E_s)$ , can be defined as

$$\hat{R}_{\text{lim}} \equiv \frac{1}{\Delta t} \frac{\hat{f}(E'|S)}{\widehat{\Delta f}(E'|S + E_s)} \quad (20)$$

whose value for large exposure becomes

$$\begin{aligned} \hat{R}_{\text{lim}}(E'|E_s) &\xrightarrow{T_{\text{total}} \rightarrow \infty} \frac{1}{\Delta t} \frac{f(E'|S)}{\Delta f(E'|S + E_s)} \\ &= \frac{1}{\Delta t} \frac{f(E'|0)}{\Delta f(E'|S + E_s)} + R_s \end{aligned} \quad (21)$$

Since  $f(E'|0)$  is non-negative everywhere,  $\lim_{T_{\text{total}} \rightarrow \infty} \hat{R}_{\text{lim}} \geq R_s$  for all  $E'$  where  $\Delta f(E'|S + E_s) > 0$  in the no pileup regime. **It is conservative for all possible background scenarios in the no pileup regime.** Of course, more complex upper limits that are constructed by weighted integration of  $\hat{R}_{\text{lim}}(E')$  taking into account the various statistical penalties [22] will also be conservative.

### D. Lack of conservativeness in the pileup regime ( $\lambda_s \gg 1$ )

In Sec. III C, we showed that when  $\lambda_s \ll 1$ ,  $\hat{R}_{\text{lim}}$  conservatively overestimates  $R_s$  for all possible background scenarios. We didn't, however, explicitly show that  $\hat{R}_{\text{lim}}$  could be non-conservative and potentially underestimate  $R_s$  in the pileup regime. Below are 2 important background scenarios in which  $\hat{R}_{\text{lim}}$  unfortunately underestimates  $R_s$ . They give us significant intuition into scenarios where we can and can not conservatively apply Eq. 21.

The absolute most challenging scenario to make conservative is one where the measured background is entirely due to dark matter interactions plus a known Gaussian noise,  $N(E'|\sigma)$ .

On the surface, this scenario is quite similar to IIB3. However, in the calibration case, we explicitly know that the peak is due to calibration events and not due to dark matter events. When seeing an unknown event peak in the dark matter search, this peak could be partially or fully a dark matter signal.

Therefore to calculate  $f(E'|S)$  we use Eq. 2 to allow for the possibility of  $m$  signal coincidences within a single time bin:

$$\begin{aligned} f(E'|S) &= \sum_{m=0}^{\infty} P(m|\lambda_s)N(E' - mE_s|\sigma) \\ &= \sum_{m=0}^{\infty} \frac{\lambda_s^m e^{-\lambda_s}}{m!} N(E' - mE_s|\sigma) \end{aligned} \quad (22)$$

1. *Non-Conservative Examples:  $\lambda_s \gg 1$  and Gaussian Noise with  $\sigma \ll E_s$*

For the limit where  $\sigma \ll E_s$ , the measured background consists of isolated quantized background peaks corresponding to  $m$  dark matter coincidences in a single time bin.  $f(E'|S + E_s)$  is found by shifting the  $f(E'|S)$  by  $E_s$

$$\begin{aligned} f(E'|S + E_s) &= f(E' - E_s|S) \\ &= \sum_{m=0}^{\infty} \frac{\lambda_s^m e^{-\lambda_s}}{m!} N(E' - (m+1)E_s|\sigma) \\ &= \sum_{m=1}^{\infty} \frac{\lambda_s^{m-1} e^{-\lambda_s}}{(m-1)!} N(E' - mE_s|\sigma) \end{aligned} \quad (23)$$

Finally, we can calculate the contaminated net differential sensitivity at  $E_s$

$$\begin{aligned} \Delta f(E'|S + E_s) &= -e^{-\lambda_s} N(E'|\sigma) \\ &+ \sum_{m=1}^{\infty} \left(1 - \frac{\lambda_s}{m}\right) \frac{\lambda_s^{m-1} e^{-\lambda_s}}{(m-1)!} N(E' - mE_s|\sigma) \end{aligned} \quad (24)$$

As shown in Fig. 4, for  $m < \lambda$  peaks,  $\Delta f(E'|S + E_s)$  is negative, while for  $m > \lambda$  it's positive. This is a true effect that's qualitatively similar to the fact that the probability

of measuring a bin with no dark matter interactions decreases as we increase the signal rate (Sec. IIB1). Integrating both  $\Delta f(E'|S + E_s)$  and  $f(E'|S)$  over the discrete peaks we find that

$$F(m|S) = \frac{\lambda_s^m e^{-\lambda_s}}{m!} \quad (25)$$

and

$$\Delta F(m|S + E_s) = \left(1 - \frac{\lambda_s}{m}\right) \frac{\lambda_s^{m-1} e^{-\lambda_s}}{(m-1)!} \quad (26)$$

for  $m \geq 1$  and generate a limit from each peak:

$$\begin{aligned} \widehat{R}_{\text{lim}}(m|E_s) &\xrightarrow{T_{\text{Total}} \rightarrow \infty} \frac{1}{\Delta t} \frac{F(m|S)}{\Delta F(m|S + E_s)} \\ &= \frac{R_s}{m - \lambda_s} \end{aligned} \quad (27)$$

and thus only the peak where  $0 \leq m - \lambda_s \leq 1$  is conservative and overestimates  $R_s$ . All peaks with  $m - \lambda_s \geq 1$  will underestimate  $R_s$  and be non-conservative.

This is both completely consistent with our general proof for conservativeness in the  $\lambda \ll 1$  limit and illustrates the natural conservativeness of standard rare event searches that set limits on signals whose deposition energy is well above the noise resolution of the detector, say  $E_s \gtrsim 3\sigma$  by looking for a non-coincident single event interaction signal.

2.  *$\lambda_s \gg 1$  with Gaussian Noise where  $\sigma \gg E_s$*

Perhaps a more pertinent and relevant scenario is when  $\lambda_s \gg 1$  and  $\sigma \gg E_s$ . In this scenario, the distributions from the various  $m$  signal event coincidences coningle and strongly overlap, and the Poissonian signal distribution can be approximated as an off-centered Gaussian distribution,  $N(E' - \lambda E_s|\sigma_s = \sqrt{\lambda_s E_s})$ . When convoluted with a non-signal normal noise distribution of unknown size,  $\sigma_?$ , one finds that

$$f(E'|S) = N(E' - \lambda_s E_s|\sigma = \sqrt{\sigma_?^2 + \lambda_s E_s^2}) \quad (28)$$

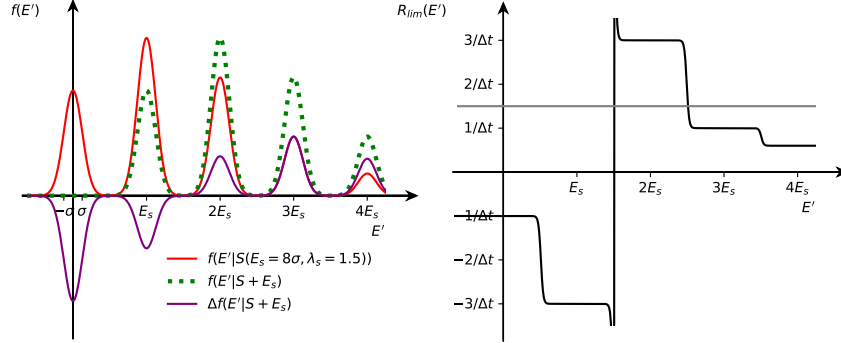


FIG. 4. Left: probability distributions for the case where there is DM contamination of the background data (see text). Here, the unknown true dark matter rate  $\lambda_s = 1.5$ , and the net response is negative at the single  $E_s$  peak. Right: limit set by eq. 27. The gray line indicates the true DM background rate. The limit is conservative only when  $1.5E_s < E' < 2.5E_s$ .

Since  $E_s$  is small with respect to the variation scale of  $f(E'|S)$ ,  $\Delta f(E'|S + E_s)$  is approximately

$$\Delta f(E'|S + E_s) \sim -\frac{\partial f(E'|S)}{\partial E'} E_s \quad (29)$$

and therefore

$$\begin{aligned} \widehat{R}_{\text{lim}} &= \frac{-1}{\Delta t E_s} \frac{f(E'|S)}{\frac{\partial f(E'|E_s)}{\partial E'}} \\ &= \frac{-1}{\Delta t E_s} \frac{1}{\frac{\partial \ln f(E'|S)}{\partial E'}} \end{aligned} \quad (30)$$

Plugging in Eq.28, we find that

$$\widehat{R}_{\text{lim}}(E'|E_s) \xrightarrow{T_{\text{Total}} \rightarrow \infty} \frac{\sigma_\gamma^2}{\Delta t E_s (E' - \lambda_s E_s)} + \frac{R_s}{\frac{E'}{E_s} - \lambda_s} \quad (31)$$

and we end up again with the unfortunate conclusion that if the Gaussian noise is dominated by Poissonian noise fluctuations of the signal (i.e.,  $\sigma_\gamma^2 \ll \lambda_s E_s^2$ ), then  $R_{\text{lim}}(E'|E_s)$  will underestimate  $R_s$  by the factor  $\frac{E'}{E_s} - \lambda_s$ . This explicit test case really highlights the most important scenario for which using the net linear differential signal response (Eq. 21) to set an upper

limit can be non-conservative; high signal pileup ( $\lambda_s \gg 1$ ) is largely indistinguishable from noise fluctuations and thus there is no way to determine if the signal is being boosted by true noise/background instead of other pileup signal interactions when  $E_s \ll \sigma$ . To both determine the relevant conservative range precisely and set conservative limits on signals where  $E_s \ll \sigma$ , we suggest using methods that set signal limits based upon the noise distribution itself [17].

#### IV. GENERALIZATION TO A SPECTRUM OF ENERGY DEPOSITION

In the previous two sections, we have worked with the case where the putative signal was expected to deposit a single true energy in the detector, e.g., to take the example of DM, a simple Bosonic DM interaction. This simplified the calculation and allowed us to gain intuition. In this section, we extend the discussion to the general case of DM interactions with a continuous true energy deposition spectrum.

### A. The case for a generic dark matter interaction

Before we consider a generic DM interaction, let us first consider the signal model of multiple discrete true energies  $E_{si}$ , with rate  $R_{si}$  respectively. We would have to take into account not only the pile-ups between the same energies as in Eq. 5, but also pile-ups between different energy  $E_{si}$  and  $E_{sj}$ , and triple pile-ups between  $E_{si}$ ,  $E_{sj}$  and  $E_{sk}$ , and so on. The formulae get rapidly out of hand but we can notice that any of these pile-up terms are at least of order two either in  $R_{si}\Delta t \equiv \lambda_{si}$  or products of several rates  $\lambda_{si}$ ,  $\lambda_{sj}$ , ..., which are also at least of order

two in rates. Therefore, if we limit ourselves to the first-order terms in rates, which is the case of negligible pile-ups, Eq. 7 becomes

$$\begin{aligned} f(E'|S(\{E_{si}, R_{si}\})) \\ = f(E'|0) + \sum_i R_{si}\Delta t(f(E'|E_{si}) - f(E'|0)) \end{aligned} \quad (32)$$

Now, in the no pile-up approximation, for interaction processes that produce a continuum of energy depositions/signal magnitudes as found in DM scattering, one can easily generalize Eq. 7 and Eq. 32 by simply integrating over the true energy,  $E_s$ :

$$f(E'|S(M_s, \sigma_s)) = f(E'|0) + \Delta t \int dE_s \frac{dR}{dE_s}(E_s|S(M_s, \sigma_s)) \left( f(E'|0 + E_s) - f(E'|0) \right) + \dots$$

where  $\frac{dR}{dE_s}(E_s|S)$  is the differential rate of DM with mass  $M_s$  at the true but unknown cross-section  $\sigma_s$ . The common practice is to calculate DM spectrum shape  $\frac{dR}{dE_s}(E_s|S)/R(S)$  at an arbitrary reference cross-section  $\sigma_0$ , and move the linear dependence on  $\sigma_s$  to the total signal rate  $R_s(S(M_s, \sigma_s))$ :

$$\begin{aligned} f(E'|S(M_s, \sigma_s)) \\ = f(E'|0) + R_s(S(M_s, \sigma_s))\Delta t \int dE_s \frac{dR}{dE_s}(E_s|S(M_s, \sigma_0)) \left( f(E'|0 + E_s) - f(E'|0) \right) + \dots \quad (33) \\ = f(E'|0) + R_s\Delta t\Delta f(E'|0 + s(M_s)) + \dots \end{aligned}$$

$f(E'|0 + E_s)$  has the same meaning as  $f(E'|E_s)$  in Sec. II A, and we use the '0+' to emphasize that  $f(E'|0 + E_s)$  is generated from a noise+background distribution without any potential signal contamination. In essence, in Eq. 33 we are simply weighting the various  $\Delta f(E'|0 + E_s)$  by the shape of the true recoil spectrum to calculate  $\Delta f(E'|0 + s(M_s))$ , the net differential sensitivity for a single elastic scatter with mass  $M_s$ .  $s(M_s)$  is the generalization of

salting with a true energy deposition  $E_s$  where one salts with true energy deposition distribution whose shape is parameterized by the DM mass,  $M_s$ . As with Eq. 6, this equation is only valid in the limit of a minimal signal pileup, ( $\lambda_s = R_s\Delta t \ll 1$ ).

Just as for the case of Bosonic DM, for small  $\lambda_s$ , one can use measurements of the potential signal contaminated search distributions to estimate the true net differential signal sensitivity as well

$$\begin{aligned}
f(E'|S(M_s, \sigma_s)) &= f(E'|0) \\
&+ R_s(S(M_s, \sigma_s))\Delta t \int dE_s \frac{\frac{dR}{dE_s}(E_s|S(M_s, \sigma_0))}{R(S(M_s, \sigma_0))} \left( f(E'|S(M_s, \sigma_s) + E_s) - f(E'|S(M_s, \sigma_s)) \right) + \dots \\
&= f(E'|0) + R_s\Delta t \Delta f(E'|S(M_s, \sigma_s) + s) + \dots
\end{aligned} \tag{34}$$

This equation can be understood as the generalization of Eq. 19. And the DM signal upper limit can be estimated in the same form as Eq. 20.

What is interesting is that Eq. 34 is not the equation used to calculate  $\frac{dR}{dE'}$  in recent noise boosting analyses. Instead the CPDv1 DM search [11], the EDELWEISS search [14], and the CRESST searches [21], have all used

$$f_{\text{bad}}(E'|S(M_s, \sigma_s)) = f(E'|0) + R_s(S(M_s, \sigma_s))\Delta t \int dE_s \frac{\frac{dR}{dE_s}(E_s|S(M_s, \sigma_0))}{R(S(M_s, \sigma_0))} f(E'|S(M_s, \sigma_s) + E_s) \tag{35}$$

They are not taking into account the fact that as  $R_s$  increases, the amount of time in which noise is non-coincident with DM signal decreases. As we will see below, **not taking this into account can lead to several non-physical effects and is certainly not conservative when there is overlap between  $f(E'|S)$  and**

$f(E'|S + E_s)$ . The ad-hoc correction being applied to this bad boosting method is to set the boosted energy  $E'$  no more than  $3\sigma$  higher than the true energy  $E$ . Since  $f(E'|S + E_s)$  can be well approximated by a Gaussian within  $\pm 3\sigma$  around  $E' - E_s = 0$ , the corrected boosting can be written as

$$\begin{aligned}
&f_{3\sigma\text{lim}}(E'|S(M_s, \sigma_s)) \\
&= f(E'|0) + R_s(S(M_s, \sigma_s))\Delta t \int dE_s \frac{\frac{dR}{dE_s}(E_s|S(M_s, \sigma_0))}{R(S(M_s, \sigma_0))} \frac{1}{\sqrt{2\pi}\sigma} e^{-\frac{(E' - E_s)^2}{2\sigma^2}} H(E_s + 3\sigma - E')
\end{aligned} \tag{36}$$

The effects of all three boosting methods are shown in the next section.

## B. Simulated Light Mass Dark Matter Search

In order to give a semi-realistic example of what a dark matter search could look like, we explore a scenario with 50 MeV Dark matter from a standard halo velocity distribution that interacts via scalar nuclear scattering with a  $5.6 \times 10^{-33} \text{ cm}^2$  cross section with a 10g Si detector that has an intrinsic Gaussian noise of

$1 \text{ eV}_{\text{rms}}$ . The same event and backgrounds are observed with two different integration times, one at 100  $\mu\text{s}$  per frame and one  $\times 100$  slower, at 10 ms per frame. The resulting difference in  $\lambda_s$  creates drastically different measured experimental differential rates and transitions us from having noise-boosted limits that are guaranteed to be conservative (Sec. III C) to the high pileup regime where it's possible that the derived limits could be non-conservative (Sec. III D).

The true energy differential signal rate,  $\frac{dR}{dE}(E|S(M_s, \sigma_n))$ , where  $S$  represents the unknown signals from DM of  $M_s = 50 \text{ MeV}$  and  $\sigma_n = 5.6 \times 10^{-33} \text{ cm}^2$ , is shown in Fig. 5 scaled

by the integration time  $\Delta t$ . We explicitly note that unlike  $\frac{dR}{dE'}(E')\Delta t = f(E')$  that has an integral of 1, the integral of  $\frac{dR}{dE}(E|S)\Delta t$  is  $\lambda_s$  and therefore is not a probability distribution function. The signal cross section was purposefully chosen such that  $\lambda_s = 0.02$  for the detector with the faster integration time (left) and 2.0 for the detector with the slower integration time (right). The true energy background differential rate,  $\frac{dR}{dE}(E|B)$ , was chosen to be qualitatively similar in shape to the low energy excess [3] commonly seen in the current generation light mass dark matter calorimeters but scaled to not completely dominate the signal. Specifically, we use the shape described by eq. 10, with  $\tau = 2 \text{ eV}$ ,  $\alpha = 1 \times 10^{-3} \text{ s}^{-1} \text{ eV}^{-1}$ , and  $\beta = 5 \times 10^{-6} \text{ s}^{-1} \text{ eV}^{-1}$ .

Next, we construct the experimentally measured probability with signal and background events hitting the detector,  $f(E'|S)$  (red). For the fast integrating detector,  $\lambda_s$  is small, and the first order Taylor expansion formulation, Eq.34, can be used. For the slowly integrating detector, a continuum true energy deposition generalized form of Eq. 4 is needed since there is significant signal pileup. To highlight the changes in the spectrum from the signal interaction, we also plot the unmeasurable background-only distribution,  $f(E'|0)$  (yellow).

The high energy tail of  $f(E'|S)$  and  $f(E'|0)$  for both detectors is simply a convolution of the noise point spread function ( $\sigma = 1 \text{ eV}$ ) with the true  $\frac{dR}{dE}(E|B)$ . Since the background event distribution is relatively slowly varying compared to the noise energy scale,  $f(E'|S)$  and  $f(E'|0) \sim \frac{dR}{dE}(E|B)\Delta t$  in the high energy range.

At low measured energies, there are substantial differences in the performance of the two detectors. For the quick detector, differences between  $f(E'|S)$  and  $f(E'|0)$  do exist but are difficult to see since only 2% of the bins have a signal interaction, and even then, a single signal interaction event has an average energy deposition  $\sim \sigma$ . For the slow detector, however, there is a significant noise broadening for  $f(E'|S)$  due to DM signal shot noise as derived and discussed in Sec. IIID 2 compared to  $f(E'|0)$

Positive portions of the linear net differential

sensitivity for DM nuclear scattering (Eq. 34) with  $M_s = 50 \text{ MeV}$  is shown in black. For comparison, the dotted black spectrum is boosted with the bad Eq. 35, which fails to consider the time occupancy by signals in coincidence with backgrounds. At all  $E'$ , this incorrect differential sensitivity estimate overestimates experimental sensitivity. In particular, above 10 eV where the backgrounds are relatively flat (Sec. IIB 4), it overestimates sensitivity by orders of magnitude. The dashed black spectrum is boosted by a simple Gaussian with  $3\sigma$  cutoff (Eq. 36), which is the conventional non-rigorous method adapted by many collaborations to avoid sensitivity to zero mass DM. Above  $\sim 4 \text{ eV}$  ( $4\sigma$ ), this method drastically underestimates the true sensitivity compared to the  $\Delta f(E'|S + s)$ ; it's too conservative. Below 4 eV ( $4\sigma$ ), however, this attempted protection isn't sufficient, and the experimental sensitivity is still overestimated.

Finally, we can look at the expectation of the derived limit using the three boosting methods. As shown in fig. 6, the expectation of  $R_{\text{lim}}$  is conservative and over-estimates  $R_s$  over the entire range of  $E'$  when  $\lambda_s \ll 1$  **for this specific signal and background scenario** when one uses both the net differential sensitivity,  $\Delta f$ , and for both the incorrect sensitivities. Of course, for experimental scenarios with even smaller backgrounds, only  $\Delta f$  estimators are guaranteed to be conservative in the small signal pileup limit. We note that for this specific scenario, the  $3\sigma$  boost constraint is conservative for  $\gtrsim 3 \text{ eV}$  ( $3\sigma$ ). This likely suggests that [11] is in fact conservative since the trigger threshold is  $4.5\sigma$ , but we emphasize this is a non-rigorous claim from a small sampling of the noise/signal/background parameter space.

For the slow detector with  $\lambda_s = 2$ , unfortunately, all 3 scenarios have energy ranges over which the derived limits are too strict and are thus **not** conservative. This case study once again explicitly demonstrates the perils of using linear net differential rate estimators when the true signal is not guaranteed to be in the  $\lambda_s \ll 1$  regime (sec. IIID 2).

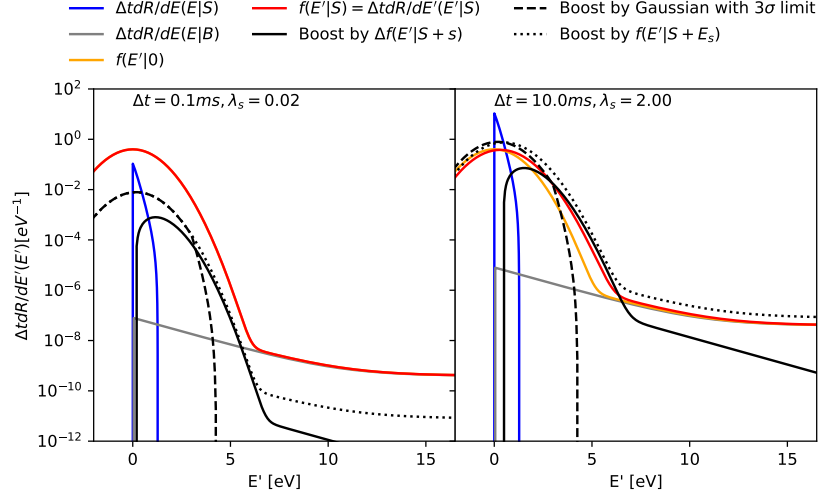


FIG. 5. A realistic detector background spectrum without dark matter, yellow,  $f(E'|0)$ , and with the presence of unknown dark matter signals, red,  $f(E'|S)$ . The background spectrum, gray, follows Eq. 10 with  $\sigma = 1 \text{ eV}$ ,  $\tau = 2 \text{ eV}$ ,  $\alpha = 1 \times 10^{-3} \text{ s}^{-1} \text{ eV}^{-1}$ , and  $\beta = 5 \times 10^{-6} \text{ s}^{-1} \text{ eV}^{-1}$ . The unknown signal, blue, is from 50MeV nuclear recoil dark matters with  $\sigma_n = 5.6 \times 10^{-33} \text{ cm}^2$  scattering in a 10g silicon detector. The resulting expected signal per integration time,  $\lambda_s$ , is 0.02 (2) for the fast (slow) integration time. The detected DM spectrum, black, is modeled using different methods of detector response boosting. The solid black line uses the correct net differential rate change proposed in this work, Eq. 34, the dotted black line uses the bad smearing that was applied in previous works, Eq. 35, and the dashed line is smeared assuming Gaussian baseline fluctuation and limiting the boost to  $3\sigma$ , Eq. 36.

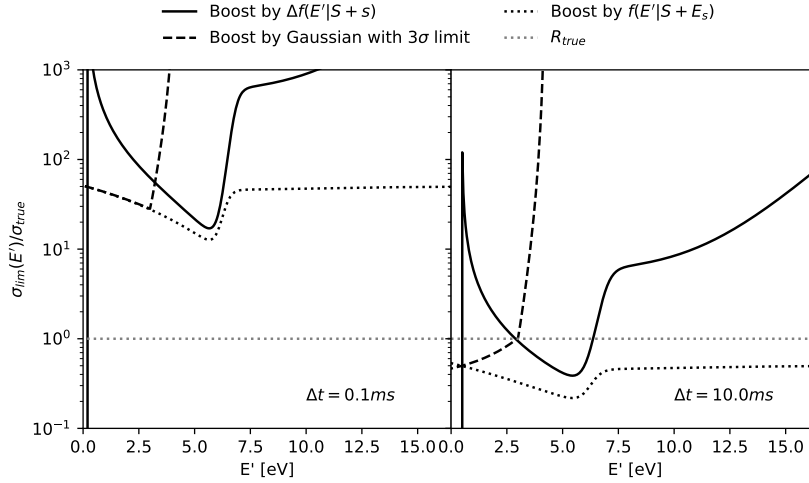


FIG. 6. Limit of DM rate with respect to the true DM background rate, assuming infinite exposure. Line styles are the same as in fig. 5. Limits in the left figure are conservative. In the right figure, long frame time results in  $\lambda_s > 1$ , and the limits are underestimated at certain  $E'$ .



## V. UNDERSTANDING ANALOG DETECTORS

So far, we have correctly calculated  $\frac{dR}{dE'}$  as a function of  $R_s$  for only an idealized time-binned detector like a CCD. In this section, we will qualitatively discuss the steps in turning a continuous time stream from an analog detector into a set of events above a trigger threshold, and show that the simplified model we developed is still qualitatively accurate. In particular, the fact that an increase in signal rate both increases the rate of noise+signal coincidence and **decreases the noise-only event rate** is simply a consequence of the fact that the total data acquisition time is fixed regardless of detector subtleties.

A modern readout that maximizes signal to noise will take an analog continuous stream of data, demix the stream if necessary, Nyquist filter, and then digitize the stream at a high enough rate that nearly the entire information content of the signal remains with high fidelity (a good rule of thumb is that the Nyquist frequency is at least  $\times 10$  larger than the fundamental dynamical poles of the signal referenced to detector output for small signals and  $\sim \times 10$  than the largest dynamical pole for optimum large signal fidelity). An acausal optimum filter or matched filter is then applied to this digitized stream to calculate a signal amplitude estimator for an event that occurs at  $t$ ,  $E'(t)$ .

A trigger algorithm will then go through this time stream and find regions where  $E' > E'_t$ , the trigger threshold energy. Each above-threshold region is then converted to a discrete number of energy depositions occurring at precise times. The simplest possible trigger algorithm, for ex-

ample, is to associate a single signal event with each above threshold region that has a signal amplitude estimator,  $E'$ , and an event time estimator,  $t'$  that occurs at the relative maximum of  $E'(t)$  in the above threshold region.

After acquiring the triggered regions, various additional selections are made to cull events that aren't consistent with high-quality signal events (pileups, saturated events, events occurring in periods of poor detector performance, events with pulse shapes inconsistent with true signal events, etc.).

### A. Optimum Filter Signal Amplitude Estimator

The simplest one time degree of freedom (DOF), one amplitude DOF optimum or matched filter [23] generates a signal amplitude estimator for an event occurring at  $t$  with the highest signal-to-noise ratio on an experimental trace,  $Y(\omega)$ , provided that:

- the noise is stationary, Gaussian distributed and characterized by a measured noise variance,  $\sigma^2(\omega)$
- the signal shape is constant for all events regardless of size and is well modeled by a template,  $T(\omega)$ .
- at most, there exists only a single event within the trace.

A derivation for the optimal estimator follows from maximizing the probability likelihood or equivalently minimizing the  $\chi^2$  of the residual

$$\chi^2 = \sum_{\omega} (Y^*(\omega) - E'T^*(\omega)e^{i\omega t}) \sigma(\omega)^{-2} (Y(\omega) - E'T(\omega)e^{-i\omega t}) \quad (37)$$

with respect to  $E'$  if the event time is known (as in the case during detector calibration with an

LED pulse) and the resulting best-fit amplitude is

$$E'(t) = \frac{\sum_{\omega} T^{\dagger}(\omega)\sigma(\omega)^{-2}Y(\omega)e^{j\omega t}}{\sum_{\omega} T^{\dagger}(\omega)\sigma(\omega)^{-2}T(\omega)} \quad (38)$$

To understand how a hypothetical true signal impacts  $E'(t)$ , we can replace  $Y$  with the sum of a noise trace,  $Y_n$ , and a true signal event that occurs at time  $t_s$  with amplitude  $E_s$  and pulse shape  $T(\omega)$  as shown graphically in Fig. 7. After Optimum filtering, we find

$$\begin{aligned} E'(t) &= \frac{\sum_{\omega} T^{\dagger}(\omega)\sigma(\omega)^{-2}(Y_n + E_s T(\omega)e^{-j\omega t_s})e^{j\omega t}}{\sum_{\omega} T^{\dagger}(\omega)\sigma(\omega)^{-2}T(\omega)} \\ &= \frac{\sum_{\omega} T^{\dagger}(\omega)\sigma(\omega)^{-2}Y_n e^{j\omega t}}{\sum_{\omega} T^{\dagger}(\omega)\sigma(\omega)^{-2}T(\omega)} + E_s \frac{\sum_{\omega} T^{\dagger}(\omega)\sigma(\omega)^{-2}T(\omega)e^{j\omega(t-t_s)}}{\sum_{\omega} T^{\dagger}(\omega)\sigma(\omega)^{-2}T(\omega)} \\ &= E'_n(t) + E_s \rho(|t - t_s|) \end{aligned} \quad (39)$$

where  $\rho(|t - t_s|)$  is the normalized weighting function which encapsulates how a true signal at  $t_s$  affects  $E'$  at  $t$ .  $\rho$ 's behavior largely depends upon the precise noise and template used. However, there are 2 completely general properties. First, at  $t = t_s$ ,  $\rho(0) = 1$ . Secondly,  $|\rho(|t - t_s|)| \leq 1$  for all  $t$ . The former means that when estimating  $E'(t = t_s)$  the filter behaves like the perfect simplistic discrete integrator:  $E'(t_s) = E'_n(t_s) + E_s$ . For all other  $t$  ( $t \neq t_s$ ), the effect of the signal is attenuated.

If the noise and template have no peaks in the frequency space, then additionally  $\rho(|t - t_s|)$  decreases monotonically with  $|t - t_s|$  as seen in Fig. 7. For these models,  $\rho(|t - t_s|)$  effectively defines a natural effective digitization scale  $\Delta t_{OF}$  below which the noise and signal qualitatively sum, and above which the change is qualitatively negligible. This behavior is qualitatively similar to the boxcar function response seen in the idealized CCD.

Somewhat surprisingly,  $\rho(t)$  is also the Pearson correlation coefficient (the normalized autocorrelation function) for the optimum filtered traces, and thus  $\rho$  is a measurement of the correlation time scale on  $E'_n(t)$ : for  $|t_1 - t_2| < \Delta t_{OF}$ ,  $E'_n(t_1)$  and  $E'_n(t_2)$  are strongly correlated. For  $|t_1 - t_2| > \Delta t_{OF}$ ,  $E'_n(t_1)$  and  $E'_n(t_2)$  are weakly correlated. This is again qualitatively like the idealized CCD where the noise in the  $j$  and  $j+1$

bins are uncorrelated. In summary, an analog detector acts qualitatively similar to the idealized integrating detector with an effective  $\Delta t_{OF}$  and thus the intuition that we developed with idealized integrating detectors is still valid.

There are two more non-intuitive deviations that we regularly encounter when implementing optimum filters. First, as foreshadowed above, sharp peaks at a given frequency in the noise or signal template, for example, a large 60Hz peak due to EMI pickup, will produce a  $\rho(|t - t_s|)$  that is non-monotonic and has multiple relative minima or ‘‘echoes’’. Secondly, we regularly find that our DC noise is significantly larger than our AC noise terms. In fact, we usually artificially set the DC noise to  $\infty$  to minimize propagation of very long time scale changes in the detector equilibrium into our energy estimator. This lack of a DC term in the optimum filter means that the time average of the weighting function,  $\langle \rho(|t - t_s|) \rangle_t = 0$ . Consequently,  $\langle \rho(|t - t_s| \gg \Delta t_{OF}) \rangle < 0$ ; counter-intuitively, the addition of a positive true signal far from a noise peak will actually slightly decrease  $E'$ .

## B. Choosing Trace Length for the Optimum Filter

To our knowledge, there isn't a clear optimization strategy for choosing the trace length,

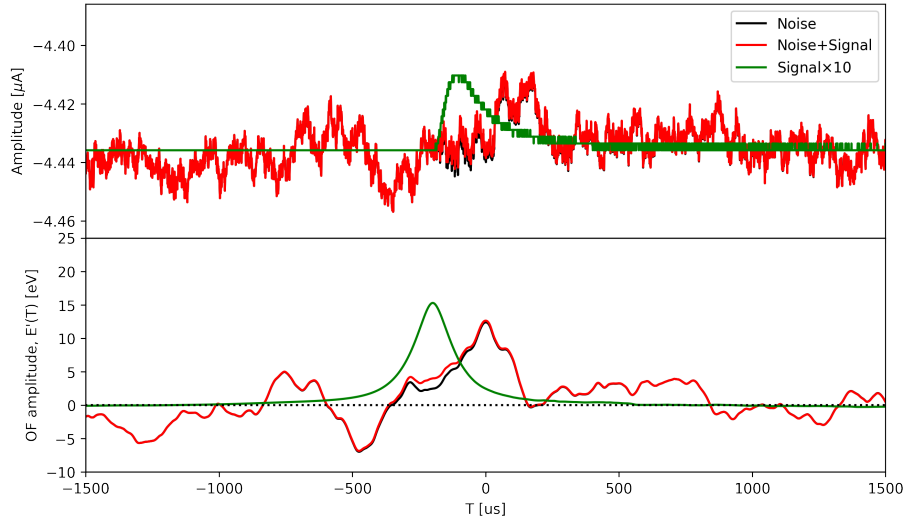


FIG. 7. A small true signal event (green, scaled by 10) is in coincidence with various noise fluctuations (black), producing the summed coincidence trace (Red). The top panel shows traces before optimal filtering, while the bottom panel displays the traces after optimal filtering. In the bottom panel, the black trace is  $E'_n(t)$  and the green trace is  $E_s\rho(|t-t_s|)$  (scaled by  $\times 10$ ). Finally, the red curve is the optimum filter output of the salted trace, which shows the behavior that we derived in eq. 39.

$T_{\text{trace}}$ , used in generating the Optimum filter. On the one hand, larger  $T_{\text{trace}}$  gives one greater frequency sensitivity and thus the optimum filter has improved ability to optimally weight different frequencies for improved sensitivity which is extremely useful in removing sharp environmental noise peaks like 60 Hz. On the other hand, larger trace lengths mean a higher probability of pileup of both signal and background events which breaks one of the assumptions required for optimality of the estimator. Thus, the total background rate and the needed calibration rate set a soft upper bound on  $T_{\text{trace}}$  since having  $1/T_{\text{trace}} \gtrsim$  to the signal+background+calibration rate will significantly increase the complexity and/or the live time loss. Consequently,  $T_{\text{trace}}$ , is commonly chosen to be the shortest possible length that doesn't significantly degrade the resolution (by say  $\sim 5\%$ ).

### C. Estimating Event Time In Trigger Algorithm

Finally and most importantly, the distillation of  $E'(t)$  into an event time estimate has no direct analog in an integrating detector and thus it unfortunately adds significant additional complexity that must be at least qualitatively understood. If neither the event time nor amplitude is known for the signal, the  $\chi^2$  is minimized with respect to both  $E'$  and  $t$ . Since  $\frac{\partial \chi^2}{\partial t} = 0$  occurs at the relative extrema of  $E'(t)$ , the standard event time estimation is at the maximum  $E'(t)$  in some fixed time window  $T_{\text{merge}}$  after the trigger goes above the trigger threshold.

We want to specifically emphasize that selecting the maximum from a random distribution is an explicitly non-linear algorithm and thus its effects must be at minimum qualitatively modeled and understood. Since only one event is recorded within the  $T_{\text{merge}}$  window, the larger the  $T_{\text{merge}}$ , the higher the probability of not triggering on an event, and thus in some

ways  $T_{\text{merge}}$  acts as dead time. However, it is truly qualitatively different than a hardware-enforced trigger dead period; bigger events are more likely to be tagged and smaller events are more likely to be untagged either due to pileup with a larger event or a larger noise fluctuation within the merge window. Minimizing these effects would suggest a smaller  $T_{\text{merge}}$  on the scale of  $\Delta t_{\text{OF}}$ . On the other hand, a  $T_{\text{merge}} \sim \Delta t_{\text{OF}} \ll T_{\text{trace}}$  will have multiple echoes of large pulses tagged as events outside the merge window if the filter is purposefully deweighting noise peaks; there is no perfect choice for simplistic trigger algorithms.

As an intermediate step to full modeling of an analog detector with an optimum filter trigger, let's follow [14] and qualitatively model the effects of the trigger algorithm searching for the maximum  $E'$  throughout a  $T_{\text{merge}}$ . To do this, we will take our idealized integrating detector, but rather than store the measured signal in every bin, we will instead store only the maximum measured energy in every  $N$  adjacent bins, which models a  $T_{\text{merge}} = N\Delta t_{\text{OF}}$ . For simplicity, we will also assume that the signal pileup probability,  $\lambda_s = R_s\Delta t_{\text{OF}}$ , is small.

Redoing our original derivation for  $\frac{dR}{dE'}$  in Eq. 2 with a  $T_{\text{merge}}$  window, we find

$$\begin{aligned} \frac{dR}{dE'}(E'|S(E_s, R_s)) &\approx \frac{1}{N\Delta t_{\text{OF}}} (P(0|R_s N\Delta t_{\text{OF}})f_{\text{max}}(E'|0) + P(1|R_s N\Delta t_{\text{OF}})f_{\text{max}}(E'|E_s)) \\ &\approx \frac{1}{N\Delta t_{\text{OF}}} ((1 - R_s N\Delta t)f_{\text{max}}(E'|0) + (R_s N\Delta t)f_{\text{max}}(E'|E_s)) \\ &\approx \frac{1}{N\Delta t_{\text{OF}}} f_{\text{max}}(E'|0) + R_s (f_{\text{max}}(E'|E_s) - f_{\text{max}}(E'|0)) \end{aligned} \quad (40)$$

where  $f_{\text{max}}(E'|0)$  is the probability distribution of the maximum of the measured energies in  $N$  bins, none of which have a signal interaction. Though it can be calculated directly, it's perhaps easiest to first calculate its cumulative distribution function, which is the probability that each and every bin has as energy  $< E'$

$$F_{\text{max}}(E'|0) = F(E'|0)^N \quad (41)$$

where  $F(E'|0)$  is the CDF of the individual bin energy distribution with no signal events and therefore

$$\begin{aligned} f_{\text{max}}(E'|0) &= \frac{dF_{\text{max}}(E'|0)}{dE'} \\ &= Nf(E'|0)F(E'|0)^{N-1} \end{aligned} \quad (42)$$

In these equations (41 and 42) we have made the simplifying assumptions that the  $E'$  measurement in different  $\Delta t_{\text{OF}}$  intervals are independent and that the signal appears only in one of

these intervals. This is approximately true with our choice of the time interval  $\Delta t_{\text{OF}}$ .

In Fig. 8,  $f_{\text{max}}(E'|0)$  is shown for a wide variety of merge window sizes for a normally distributed  $f(E'|0)$ . For  $E'$  where  $F(E'|0) < N^{-1/(N-1)}$ ,  $f_{\text{max}}(E'|0) < f(E'|0)$  and this suppression of low energy events increases with  $N$ . Simply put, to have a low-energy event in the maximum distribution requires a low-energy event in every bin. On the other hand, the probability of sampling a higher outlier tail event goes up substantially: in the limit as  $F(E'|0) \rightarrow 1$ ,  $f_{\text{max}}(E'|0) = Nf(E'|0)$ .

Likewise,  $F_{\text{max}}(E'|E_s)$  can be derived by recognizing that the bin with the signal event and the  $N - 1$  bins without the signal event must all have energies  $< E'$ ,

$$F_{\text{max}}(E'|E_s) = F(E'|E_s)F(E'|0)^{N-1} \quad (43)$$

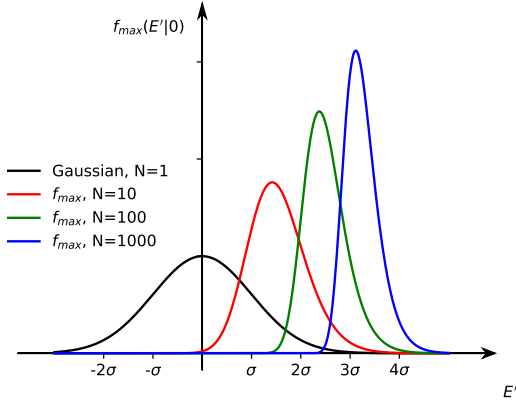


FIG. 8. A normally distributed  $f(E'|0)$  in black, and the resultant  $f_{\max}(E'|0)$  for  $N = 10$  (red), 100 (green), and 1000 (blue)

and therefore

$$\begin{aligned} f_{\max}(E'|E_s) &= \frac{dF_{\max}(E'|E_s)}{dE'} \\ &= f(E'|E_s)F(E'|0)^{N-1} \\ &+ F(E'|E_s)(N-1)f(E'|0)F(E'|0)^{N-2} \end{aligned} \quad (44)$$

Because only the maximum of the  $N$  bins is stored, there is a substantial probability that a time bin with a true signal whose amplitude is small compared to the noise fluctuation (i.e., when  $F(E_s|0) < 1$ ) will be unrecorded because there will be a larger noise fluctuation in one of the other  $N-1$  bins. By contrast, for large amplitude signals,  $F(E_s|0) \approx 1$ ,  $f_{\max}(E'|E_s) \approx f(E'|E_s)$ .

Writing the measured differential rate (Eq. 40) in terms of  $f(E'|0)$  using Eq. 42 and 44 we find

$$\begin{aligned} \frac{dR}{dE'}(E'|S) &= \frac{1}{\Delta t_{\text{OF}}} f(E'|0)F(E'|0)^{N-1} \\ &+ R_s F(E'|0)^{N-1} \left( [f(E'|E_s) - f(E'|0)] + [F(E'|E_s) - F(E'|0)] \frac{(N-1)f(E'|0)}{F(E'|0)} \right) \end{aligned} \quad (45)$$

Due to the facts that  $F(E'|0)^{N-1} < 1$  and  $[F(E'|E_s) - F(E'|0)] < 0$  always, the net differential sensitivity is always suppressed by a large merging window, though, of course, the sensitivity loss is most egregious for small signals. Consequently, we strongly recommend one uses the smallest feasible merge window when searching for signals that comingle with noise. However, when searching for large signals where there is no overlap with the noise distribution as occurs in high mass dark matter searches when  $F(E_s|0) \sim 1$  Eq. 40 simplifies back to the expected

$$\begin{aligned} \lim_{F(E_s|0) \rightarrow 1} \frac{dR}{dE'}(E'|S) \\ = \frac{1}{\Delta t_{\text{OF}}} f(E'|0) + R_s f(E'|E_s) \end{aligned} \quad (46)$$

## VI. MEASURING POTENTIALLY CONTAMINATED NET DIFFERENTIAL SIGNALS IN ANALOG DETECTORS WITH SALTING

In Sec. III, we showed that conservative limits on signal interaction rates could be estimated from the **measurable** potentially signal contaminated background distribution  $f(E'|S)$  and the measurable potentially contaminated net differential signal sensitivity  $\Delta f(E'|S + E_s) = f(E'|S + E_s) - f(E'|S)$  for an idealized integrating detector. Then in Sec. V, we showed that analog detectors with a continuous time stream were qualitatively similar to the idealized integrating detectors and thus all of our intuition remains intact and we should be able to follow a similar procedure to produce conservative signal rate limits. Unfortunately, the quantitative de-

tailed differences require a change in approach. Specifically:

- In analog detectors, the correlation time  $\Delta t_{\text{OF}}$  and even the concept of coincidence are qualitative concepts. Consequently, the simplistic relationship that  $\frac{dR}{dE'} = \frac{1}{\Delta t} f(E')$  is not rigorously correct. As a consequence, we will work directly with the differential rates such as  $\frac{dR}{dE'}(E'|S)$ .
- Triggering and merging algorithms are all fundamentally non-linear. As a result,  $\frac{dR}{dE'}(E'|S + E_s) \neq \frac{dR}{dE'}(E' - E_s|S)$ . In Sec. V, we did produce a qualitatively accurate, but very simplistic model of these non-linear effects for a specific trigger algorithm but using this model for sensitivity estimates would certainly incur some systematic modeling error.

What remains true for analog detectors is that the dependence of the search differential rate,  $\frac{dR}{dE'}(E'|S)$ , on the signal rate can be Taylor expanded to first order in the signal rate as long as **the true signal pileup rate is small**:

$$\begin{aligned} & \frac{dR}{dE'}(E'|S(\{R_{si}, E_{si}\})) \\ &= \frac{dR}{dE'}(E'|0) + \sum_i R_{si} \Delta f(E'|0 + E_{si}) \end{aligned} \quad (47)$$

Here, we have again made explicit that  $S$  describes the potential superposition of signals of various true energies (the sum can also include integration over true energies). This expresses that, in the non-pileup limit, both the increase in measured energy differential rate and the dead time it imposes on the noise and background differential rate are both proportional to  $R_{si}$ . The constant of proportionality is as before, the net differential sensitivity for a signal of that true energy. We kept for it the same notation,  $\Delta f(E'|0 + E_{si})$ , although it is no longer a difference between  $f$ 's.

Following the same logical arguments that led to Eq. 19 and 34, we show that salting the signal contaminated search data can be used to

estimate  $\Delta f(E'|0 + E_{si})$  with an accuracy sufficient for approximation to first order in the rate used in Eq. 47.

Specifically, let us add a known random rate  $r_s$  of events with true energy  $E_s$  **to the raw analog search data stream before the triggering algorithm**. To first order in rates, the salted events behave in the same way as the signal events  $S_i$  and Eq. 47 becomes

$$\begin{aligned} & \frac{dR}{dE'}(E'|S(\{R_{si}, E_{si}\}) + s(r_s, E_s)) \\ &= \frac{dR}{dE'}(E'|0) + \sum_i R_{si} \Delta f(E'|0 + E_{si}) \\ &+ r_s \Delta f(E'|0 + E_s) \\ &= \frac{dR}{dE'}(E'|S(\{E_{si}, R_{si}\})) + r_s \Delta f(E'|0 + E_s) \end{aligned} \quad (48)$$

Therefore, to first order in signal rates the net differential sensitivity

$$\begin{aligned} \Delta f(E'|0 + E_s) &= \frac{\frac{dR}{dE'}(E'|S + s) - \frac{dR}{dE'}(E'|S)}{r_s} \\ &\equiv \Delta f(E'|S + E_s) \end{aligned} \quad (49)$$

$\Delta f(E'|S + E_s)$  is the salting-derived net differential sensitivity, which can be estimated from the salting rate normalized difference between the measured salted and unsalted differential rates:

$$\widehat{\Delta f}(E'|S + E_s) = \frac{\widehat{\frac{dR}{dE'}}(E'|S + s) - \widehat{\frac{dR}{dE'}}(E'|S)}{r_s} \quad (50)$$

This result makes intuitive sense. The difference between the post-analysis differential rates between the salted and non-salted searches is the net effect of the salted signal interaction. At small signal rates, the probability of pileup between salt and potential signals is negligible, and the theoretical and salted differential sensitivities are essentially the same.

This equation is valid for arbitrary  $r_s$  under the limit of  $r_s \Delta t_{\text{OF}} \ll 1$ . The choice of  $r_s$  does not affect the result, as it scales simultaneously

in the denominator and numerator of Eq. 50. It should not be confused with the potential DM signal rate  $R_s$ . In practice, a high  $r_s$  may be desired for computational efficiency. As we have full control of the salting process, one can force the Monte Carlo process to avoid salt-salt pile-up. This procedure also avoids the subtlety of estimating  $\Delta t_{\text{OF}}$ .

Notice that this salting scheme requires no definition of any *ad hoc* effective coincidence time scale. In fact, this scheme never attempts to explicitly define if the trigger is coincident or not coincident with the salted signal (which we know is a simplification since the weighting function,  $\rho$ , is a continuum and thus the concept of coincidence is also a continuum). Additionally, since the data is salted before the triggering algorithm, all subtleties, non-linearities, and quirks of this algorithm are by construction accounted for, even if the algorithm is challenging to understand.

If an estimate of the no-signal differential rate,  $\frac{dR}{dE'}(E'|0)$  is possible, then background subtracted estimators for the signal interaction rate can be constructed using Eq. 50 to estimate the  $\Delta f(E'|0 + E_s)$ .

If we do not have enough confidence to estimate no-signal differential rates, one can obtain in the no-pileup assumption a conservative upper limit for a putative signal in the following way. We salt separately for each energy. This salting will be repeated on the raw data stream (not cumulatively) to estimate  $\widehat{\Delta f}(E'|S + E_s)$  of each different  $E_s$ . Then, following Eq. 34, we convolve the net differential response of each true energy with the true DM spectrum shape to estimate  $\widehat{\Delta f}(E'|S + s(M_s))$ . Finally, we set a conservative upper limit to the DM signal rate similarly as Eq. 20.

$$\widehat{R}_{\text{lim}} \equiv \frac{\widehat{\frac{dR}{dE'}}(E'|S)}{\widehat{\Delta f}(E'|S + s(M_s))} \quad (51)$$

## VII. CONCLUSION

Previous light mass dark matter searches that set limits on dark matter interaction rates by

searching for interactions whose sub-threshold true energy depositions were boosted above threshold by being in coincidence with large positive noise fluctuations could potentially overestimate their experimental signal sensitivity because they did not account for the effect of having a decreased rate of background/noise only interactions in their detector.

Furthermore, we explicitly proved that correct estimation of the signal contaminated net differential signal sensitivity would give conservative interaction limits for all possible background scenarios, **provided that the true interaction signal rate produced minimal signal-signal pileup**. We also explicitly proved that large signal-signal pileup could indeed produce non-conservative interaction limits using this linear approximation for some background cases. Consequently, the conservativeness of this linear interaction estimate technique for signals with interactions whose average value is of the order of the noise resolution must be confirmed with measurement techniques like [17].

We also showed that analog detectors that produce a continuous time stream of data are qualitatively similar to idealized time discretized integrating detectors like CCDs in so far as there exists an effective timescale,  $\Delta t_{\text{OF}}$ , below which noise is strongly correlated and signal interactions roughly add to the noise fluctuation, and above which noise is uncorrelated and signal interactions do not affect the noise and thus all of our intuition regarding estimating interaction rates in the linear regime remain valid as long as one takes into account non-linearities introduced by the triggering algorithm. This is most easily done by salting the raw data stream.

## VIII. ACKNOWLEDGEMENTS

During the CPD analysis [10], Steve Yellin recognized and publicized internally within the SuperCDMS collaboration the fact that simply noise smearing the signal led to completely unphysical zero mass search sensitivity. This

original insight (reproduced in Sec. IIB2) directly led to and inspired this paper. Thus, even though he claims his contributions to this paper are minimal and aren't worthy of authorship, we strongly disagree. We also specifically recognize Wolfgang Rau for really pushing us to fully flesh out the ramifications of having a signal rate that had a significant pileup ( $\lambda_s \geq 1$ ). This push directly led to the realization that

for pileup signal rates, the use of the linear net differential signal model could lead to non-conservative limits. We recognize and thank the SuperCDMS, TESSERACT, EDELWEISS, and RICOCHET collaborations for insightful comments throughout the drafting process, in particular Jules Gascon, Belina von Krosigk, Scott Oser, Wolfgang Rau, and Steve Yellin. This work was supported by the NSF and DOE.

- 
- [1] J. Aalbers, D. Akerib, C. Akerlof, A. Al Musalhi, F. Alder, A. Alqahtani, S. Alsum, C. Amarasinghe, A. Ames, T. Anderson, et al. First dark matter search results from the lux-zepplin (lz) experiment. *Physical review letters*, 131(4):041002, 2023.
- [2] A. H. Abdelhameed, G. Angloher, P. Bauer, A. Bento, E. Bertoldo, C. Bucci, L. Canonica, A. D'Addabbo, X. Defay, S. Di Lorenzo, et al. First results from the cresst-iii low-mass dark matter program. *Physical Review D*, 100(10):102002, 2019.
- [3] P. Adari, A. Aguilar-Arevalo, D. Amidei, G. Angloher, E. Armengaud, C. Augier, L. Balogh, S. Banik, D. Baxter, C. Beaufort, G. Beaulieu, V. Belov, Y. B. Gal, G. Benato, A. Benoît, A. Bento, L. Bergé, A. Bertolini, R. Bhattacharyya, J. Billard, I. Bloch, A. Botti, R. Breier, G. Bres, J.-L. Bret, A. Broniatowski, A. Brossard, C. Bucci, R. Bunker, M. Cababie, M. Calvo, P. Camus, G. Cancelo, L. Canonica, F. Cappella, L. Cardani, J.-F. Caron, N. Casali, G. Castello, A. Cazes, R. Cerulli, B. C. Vergara, D. Chaize, M. Chapellier, L. Chaplinsky, F. Charlieux, M. Chaudhuri, A. Chavarria, G. Chemin, R. Chen, H. Chen, F. Chierchie, I. Colantoni, J. Colas, J. Cooley, J.-M. Coquillat, E. Corcoran, S. Crawford, M. Crisler, A. Cruciani, P. Cushman, A. D'Addabbo, J. D'Olivo, A. Dastgheibi-Fard, M. D. Jésus, Y. Deng, J. Dent, E. Depaoli, K. Dering, S. Dharani, S. D. Lorenzo, A. Drlica-Wagner, L. Dumoulin, D. Durnford, B. Dutta, L. Einfalt, A. Erb, A. Erhart, R. Essig, J. Estrada, E. Etzion, O. Exshaw, F. Favela-Perez, F. v. Feilitzsch, G. F. Moroni, N. F. Iachellini, S. Ferriol, S. Fichtinger, E. Figueroa-Feliciano, J.-B. Filippini, D. Filosofov, J. A. Formaggio, M. Friedl, S. Fuard, D. Fuchs, A. Fuss, R. Gaïor, A. Garai, C. Garrah, J. Gascon, G. Gerbier, M. Ghaith, V. Ghete, D. Gift, I. Giomataris, G. Giroux, A. Giuliani, P. Gorel, P. Gorla, C. Goupy, J. Goupy, C. Goy, M. Gros, P. Gros, Y. Guardincerri, C. Guerin, V. Guidi, O. Guillaudin, S. Gupta, E. Guy, P. Harrington, D. Hauff, S. T. Heine, S. A. Hertel, S. Holland, Z. Hong, E. Hoppe, T. Hossbach, J.-C. Ianigro, V. Iyer, A. Jastram, M. Ješkovský, Y. Jin, J. Jochum, J. P. Johnston, A. Juillard, D. Karaivanov, V. Kashyap, I. Katsioulas, S. Kazarcev, M. Kaznacheeva, F. Kelly, B. Kilminster, A. Kinast, L. Klinkenberg, H. Kluck, P. Knights, Y. Korn, H. Kraus, B. von Krosigk, A. Kubik, N. Kurinsky, J. Lamblin, A. Langenkämper, S. Langrock, T. Lasserre, H. Lattaud, P. Lautridou, I. Lawson, S. Lee, M. Lee, A. Letessier-Selvon, D. Lhuillier, M. Li, Y.-T. Lin, A. Lubashevskiy, R. Mahapatra, S. Maludze, M. Mancuso, I. Manthos, L. Marini, S. Marnieros, R. Martin, A. Matalon, J. Matthews, B. Mauri, D. W. Mayer, A. Mazzolari, E. Mazzucato, H. M. zu Theenhausen, E. Michielin, J. Minet, N. Mirabol-fathi, K. v. Mirbach, D. Misiak, P. Mitra, J.-L. Mocellin, B. Mohanty, V. Mokina, J.-P. Mols, A. Monfardini, F. Mounier, S. Munagavalasa, J.-F. Muraz, X.-F. Navick, T. Neep, H. Neog, H. Neyrial, K. Nikolopoulos, A. Nilima, C. Nones, V. Novati, P. O'Brien, L. Oberauer, E. Olivieri, M. Olmi, A. Onillon, C. Oriol, A. Orly, J. Orrell, T. Ortmann, C. Overman, C. Pagliarone, V. Palušová, P. Pari, P. K. Patel, L. Pattavina, F. Petricca, A. Piers, H. D. Pinckney, M.-C. Piro, M. Platt, D. Poda, D. Ponomarev, W. Potzel, P. Povinec, F. Pröbst, P. Privitera, F. Pucci, K. Ra-



- manathan, J.-S. Real, T. Redon, F. Reindl, R. Ren, A. Robert, J. Rocha, D. Rodrigues, R. Rogly, J. Rothe, N. Rowe, S. Rozov, I. Rozova, T. Saab, N. Saffold, T. Salagnac, J. Sander, V. Sanglard, D. Santos, Y. Sarkis, V. Savu, G. Savvidis, I. Savvidis, S. Schönert, K. Schäffner, N. Schermer, J. Schieck, B. Schmidt, D. Schmiedmayer, C. Schwertner, L. Scola, M. Settimo, Y. Shevchik, V. Sibille, I. Sidelnik, A. Singal, R. Smida, M. S. Haro, T. Soldner, J. Stachurska, M. Stahlberg, L. Stefanazzi, L. Stodolsky, C. Strandhagen, R. Strauss, A. Stutz, R. Thomas, A. Thompson, J. Tiffenberg, C. Tomei, M. Traina, S. Uemura, I. Usherov, L. Vagneron, W. V. D. Pontseele, F. V. de Sola Fernandez, M. Vidal, M. Vignati, A. Virto, M. Vivier, T. Volansky, V. Wagner, F. Wagner, J. Walker, R. Ward, S. Watkins, A. Wex, M. Willers, M. Wilson, L. Winslow, E. Yakushev, T.-T. Yu, M. Zampaolo, A. Zaytsev, V. Zema, D. Zinatulina, and A. Zolotarova. EXCESS workshop: Descriptions of rising low-energy spectra. *SciPost Phys. Proc.*, page 001, 2022. doi:10.21468/SciPostPhysProc.9.001. URL <https://scipost.org/10.21468/SciPostPhysProc.9.001>.
- [4] P. Agnes, I. F. d. M. Albuquerque, T. Alexander, A. Alton, G. Araujo, D. M. Asner, M. Ave, H. O. Back, B. Baldin, G. Batignani, et al. Low-mass dark matter search with the darkside-50 experiment. *Physical review letters*, 121(8):081307, 2018.
- [5] R. Agnese, Z. Ahmed, A. Anderson, S. Arrenberg, D. Balakishiyeva, R. Basu Thakur, D. Bauer, J. Billard, A. Borgland, D. Brandt, et al. Silicon detector dark matter results from the final exposure of cdms ii. *Physical review letters*, 111(25):251301, 2013.
- [6] R. Agnese, T. Aralis, T. Aramaki, I. Arnquist, E. Azadbakht, W. Baker, S. Banik, D. Barker, D. Bauer, T. Binder, et al. First dark matter constraints from a supercdms single-charge sensitive detector. *Physical review letters*, 121(5):051301, 2018.
- [7] A. Aguilar-Arevalo, I. Arnquist, N. Avalos, L. Barak, D. Baxter, X. Bertou, I. Bloch, A. Botti, M. Cababie, G. Canelo, et al. Confirmation of the spectral excess in damic at snolab with skipper ccds. *Physical Review D*, 109(6):062007, 2024.
- [8] D. Akerib, S. Alsum, H. Araújo, X. Bai, J. Balajthy, A. Baxter, E. Bernard, A. Bernstein, T. Biesiadzinski, E. Boulton, et al. Investigation of background electron emission in the lux detector. *Physical Review D*, 102(9):092004, 2020.
- [9] M. Albakry, I. Alkhatib, D. Amaral, T. Aralis, T. Aramaki, I. Arnquist, I. Ataee Langroudy, E. Azadbakht, S. Banik, C. Bathurst, et al. Investigating the sources of low-energy events in a supercdms-hvev detector. *Physical Review D*, 105(11):112006, 2022.
- [10] I. Alkhatib, D. Amaral, T. Aralis, T. Aramaki, I. J. Arnquist, I. Ataee Langroudy, E. Azadbakht, S. Banik, D. Barker, C. Bathurst, et al. Light dark matter search with a high-resolution athermal phonon detector operated above ground. *Physical review letters*, 127(6):061801, 2021.
- [11] I. Alkhatib, D. Amaral, T. Aralis, T. Aramaki, I. J. Arnquist, I. A. Langroudy, E. Azadbakht, S. Banik, D. Barker, C. Bathurst, et al. Light dark matter search with a high-resolution athermal phonon detector operated above ground. *Physical review letters*, 127(6):061801, 2021.
- [12] J. Angle, E. Aprile, F. Arneodo, L. Baudis, A. Bernstein, A. Bolozdynya, L. Coelho, C. Dahl, L. DeViveiros, A. Ferella, et al. Search for light dark matter in xenon10 data. *Physical Review Letters*, 107(5):051301, 2011.
- [13] R. Anthony-Petersen, A. Biekert, R. Bunker, C. L. Chang, Y.-Y. Chang, L. Chaplinsky, E. Fascione, C. W. Fink, M. Garcia-Sciveres, R. Germond, et al. A stress-induced source of phonon bursts and quasiparticle poisoning. *Nature Communications*, 15(1):6444, 2024.
- [14] E. Armengaud, C. Augier, A. Benoît, A. Benoit, L. Bergé, J. Billard, A. Broniatowski, P. Camus, A. Cazes, M. Chapellier, et al. Searching for low-mass dark matter particles with a massive ge bolometer operated above ground. *Physical Review D*, 99(8):082003, 2019.
- [15] I. Arnquist, N. Avalos, D. Baxter, X. Bertou, N. Castelló-Mor, A. Chavarria, J. Cuevas-Zepeda, J. C. Gutiérrez, J. Duarte-Campderros, A. Dastgheibi-Fard, et al. First constraints from damic-m on sub-gev dark-matter particles interacting with electrons. *Physical Review Letters*, 130(17):171003, 2023.
- [16] L. Barak, I. M. Bloch, M. Cababie, G. Canelo, L. Chaplinsky, F. Chierchie, M. Crisler, A. Drlica-Wagner, R. Essig, J. Estrada, et al.

- Sensei: Direct-detection results on sub-gev dark matter from a new skipper ccd. *Physical Review Letters*, 125(17):171802, 2020.
- [17] A. Das, N. Kurinsky, and R. K. Leane. Dark matter induced power in quantum devices. *Physical Review Letters*, 132(12):121801, 2024.
- [18] L. Hehn, E. Armengaud, Q. Arnaud, C. Augier, A. Benoît, L. Bergé, J. Billard, J. Blümer, T. De Boissiere, A. Broniatowski, et al. Improved edelweiss-iii sensitivity for low-mass wimps using a profile likelihood approach. *The European Physical Journal C*, 76:1–10, 2016.
- [19] M. Kendall and A. Stuart. *The Advances Theory of Statistics*, volume 2. Charles Griffin and Company Limited, London, 2 edition, 1967.
- [20] Z. Liu, L. Yang, Q. Yue, C. Yeh, K. Kang, Y. Li, M. Agartioglu, H. An, J. Chang, J. Chen, et al. Studies of the earth shielding effect to direct dark matter searches at the china Jinping underground laboratory. *Physical Review D*, 105(5):052005, 2022.
- [21] M. Mancuso, A. Abdelhameed, G. Angloher, R. Breier, P. Bauer, A. Bento, E. Bertoldo, C. Bucci, L. Canonica, A. D’Addabbo, et al. Searches for light dark matter with the cresst-iii experiment. *Journal of Low Temperature Physics*, 199(1-2):547–555, 2020.
- [22] S. Yellin. Finding an upper limit in the presence of an unknown background. *Physical Review D*, 66(3):032005, 2002.
- [23] L. A. Zadeh and J. R. Ragazzini. Optimum filters for the detection of signals in noise. *Proceedings of the IRE*, 40(10):1223–1231, 1952.